CHEMICAL ENGINEERING TRANSACTIONS
VOL. 84, 2021
A publication of AIDIC
The Italian Association of Chemical Engineering
Online at www.cetjournal.it
Guest Editors: Paolo Ciambelli, Luca Di Palma

ISBN 978-88-95608-82-2; **ISSN** 2283-9216

Direct Synthesis of H_2O_2 On Pd/Al_2O_3 Contactors: Understanding the Effect of Pd Particle Size and Calcination through Kinetic Analysis

Gianfranco Giorgianni[a,*], Daniela Cozza[a], Francesco Dalena[a], Emanuele Giglio[a], Salvatore Abate[b]

[a] Laboratorio di Chimica Industriale e Catalisi, Università della Calabria, Via P. Bucci, I-87036, Rende, CS, Italia
[b] Dipartimento di Scienze Chimiche, Biologiche, Farmaceutiche, ed Ambientali (ChiBioFarAM), Università degli Studi di Messina, V.le F. Stagno D'Alcontres 31, Messina 98166, Italia
gianfranco.giorgianni@unical.it

The direct synthesis of H_2O_2 on Pd-based catalysts, although recognized as a potential route for the sustainable production of H_2O_2, is still limited by the low catalytic selectivity and safety concerns. Here, the calcination treatment effect, with the dispersion of Pd NPs and its interaction with Al_2O_3, is investigated. Catalysts have been prepared by the sol-immobilization procedure (SI) on Al_2O_3 as asymmetric alumina membranes (AAS) and tested in both reduced and calcined form (450°C, 1°C/min, 8 h) for the direct synthesis of H_2O_2. Finally, the catalytic performance was compared with other catalysts, prepared by hydrazine-reduction (NRC) and impregnation-decomposition (IDC) already reported in a previous paper and calcined for a shorter time (450°C, 1°C/min, 6 h).
TEM micrographs showed the formation of Pd NPs with average diameters of 12 (NR), 3.8 (IDC), and 3.3 nm (SI), respectively. The reduced SI catalyst has shown a 2-4% selectivity. However, after calcination (SIC), a 69 % selectivity to H_2O_2 was reached. Compared with NRC and IDC catalysts, the selectivity increased within the series NRC < IDC < SIC. The kinetic analysis of calcined catalysts showed an overall decrease of the hydrogenolysis and direct combustion routes in the series NRC > IDC > SIC. The SIC catalyst's improved performance was related to the increased interaction with the support, stabilizing Pd in its oxidized form.

1. Introduction

H_2O_2 is a potential green oxidant used for environmental remediation and wastewater treatments (Bianco et al., 2009). However, the current production scenario, by the anthraquinone oxidation process, significantly impacts the environment. The direct synthesis of H_2O_2 has been reported as a potential greener substitute for the anthraquinone oxidation process (Flaherty, 2018). However, its industrialization is limited by safety concerns related to the use of H_2/O_2 mixtures in the explosion region and the catalysts' low selectivity (Centi et al., 2009). To improve safety of slurry reactors, the use of CO_2 as ballast in slurry reactors was proposed (Centi & Perathoner, 2009). Besides, microreactors (Voloshin et al., 2007), Dense Membranes of Pd (Abate et al., 2015), and Pd-Au (Iulianelli et al., 2019), traditionally employed for the separation of hydrogen, were also employed for the direct synthesis of H_2O_2, together with the use of catalytic contactors (S Abate et al., 2006). To enhance the process's selectivity and productivity, several Pd-based catalysts have been proposed, e.g., Pd/CNT, Pd/CMF (Arrigo et al., 2016), and Pd-Sn catalysts (Freakley et al., 2016). Interesting selectivity and productivity of H_2O_2 were obtained by the sol-immobilization procedure (Abate et al., 2010). In the latter case, an external protective layer of PVA, used as a capping agent, when at low concentration, has been proposed to promote the reaction (Giorgianni et al., 2019). Also, the reaction has been found to be structure sensitive (Choudhary & Jana, 2008) and, calcination treatments have been found to improve the reaction's selectivity (García-Serna et al., 2014). Even though the nature of the active site (Pd or Pd oxide) for the reaction has been under debate for a long time, it has been suggested, supported by kinetic modelling of the surface dynamics of oxidized Pd nanoparticles, that the active site can be metallic Pd (Abate et al., 2016).

In this paper, structured catalysts were prepared by sol-immobilization and tested both in the reduced and in the calcined form. The effect of the Pd NPs size and calcination treatments' duration were investigated, comparing the catalyst calcined at 450°C for 8 h with other previously published catalysts prepared by impregnation-decomposition (IDC) and hydrazine reduction (NRC) calcined at the same temperature for 6 h (Abate et al., 2016). Finally, the dynamics of the oxidation state of the calcined catalyst was investigated by kinetic analysis.

2. Experimental

2.1 Preparation of the Catalyst

Pd/Al_2O_3 structured catalysts were prepared by sol-immobilization (SI) (Giorgianni et al., 2019). A 100 mL solution containing PVA (0.28 g - Sigma-Aldrich, 363170-25G) and Na_2PdCl_4 (0.044 g) was kept under stirring conditions till solubilization of the precursor. Then, solid $NaBH_4$ (0.028 g) was quickly added to the precursor solution. After the addition of $NaBH_4$, the precursor solution turned immediately from yellow to black, highlighting the formation of a sol of metallic Pd nanoparticles (Pd NPs). After 30 min, the pH of the sol was adjusted to 2, by the addition of H_2SO_4. Finally, the acidified sol was immobilized on the internal mesoporous side of an asymmetric alumina membrane (Inopor; L: 10 cm; ϕ_{in}: 0.7 cm; average mesopore diameter: 70 nm). The obtained catalyst was rinsed with deionized water and dried at 50°C (SI catalyst). A second catalyst was calcined at 450°C (8h, 1°C/min) and identified as SIC in the text. The preparation of the benchmark catalysts by hydrazine reduction (NRC) and impregnation-decomposition (IDC), both calcined at 450°C for 6 h (1°C/min), was reported in a previous paper (Abate et al., 2016).

2.2 Characterization

A CM12 Microscope (Philips) recorded the TEM micrograph of the prepared catalyst (SiC). The internal surface of the structured catalyst, where Pd was deposited, was gently scratched. The resulting powder was dispersed in 2-propanol and then deposited on the surface of a holey-carbon-film supported copper grid. Average Pd NPs diameters were calculated after measuring at least 200 nanoparticles.
A Perkin-Elmer Analyst 200 atomic absorption spectrometer (AAS) measured the loading of the prepared catalyst. The prepared catalyst, before calcination, was digested in Aqua Regia.

2.3 Testing

The prepared catalyst was tested in a recirculated semi-batch contactor reactor described in a previous paper (Abate et al., 2016) for four hours. Methanol (100 mL) was used as a solvent in the presence of KBr (0.06g) and H_2SO_4 as promoters (100 µL 96% H_2SO_4). H_2 (purity 5.0) was fed continuously from the catalytic contactor's outer side, and its gauge pressure was fixed at 2.0 ± 0.1 bar by using a pressure regulator. The consumption of H_2 was measured using a Thermal Mass Flow Meter (Bronkhorst). O_2 (purity 5.0) was continuously bubbled (70 mL_{nc}/min) within the methanol solution at atmospheric pressure using a Thermal Mass Flow Controller (Brooks Instruments). Before each test, the testing solution was pre-saturated with O_2 for 20 min. Liquid samples were taken from the reactor and measured for the concentration of H_2O and H_2O_2. An automatic titrator (794 Basic Titrino, Metrohm) measured the concentration of H_2O_2 by iodometric titration, a KF Coulometric apparatus (Metrohm 831 KF coulometer) measured the concentration of water. The water formed during the tests was calculated by subtracting the methanol solution's initial water concentration. The selectivity of the catalyst toward H_2O_2 ($S_{H_2O_2}(\mathrm{t})$) was calculated by Eq(1) (see symbols definitions and units at the end of the text). The conversion of H_2 ($\varepsilon^t_{H_2}(\mathrm{t}_0,\mathrm{t})$) was calculated by the ratio of the sum of the produced H_2O and H_2O_2 and the fed H_2 ($\dot{n}_{H_2}(t)$) (Eq(2)).

$$S_{H_2O_2}(\mathrm{t}) = \frac{c_{H_2O_2}(\mathrm{t})}{c_{H_2O_2}(\mathrm{t}) + c_{H_2O}(t)} \tag{1}$$

$$\varepsilon^t_{H_2}(\mathrm{t}_0,\mathrm{t}) = \frac{\left|c_{H_2O_2}(\mathrm{t}) + c_{H_2O}(t)\right|_{t_0}^{t} \cdot V_{sln}}{\int_{t_0}^{t} \dot{n}_{H_2}(t) \cdot dt} \tag{2}$$

3. Results and Discussion

3.1 Characterization

The obtained average Pd NPs size for the uncalcined catalysts was reported in Table 1, together with their respective Pd loading, as calculated by AAS, and compared with catalysts prepared by hydrazine reduction

(NRC) and impregnation-decomposition (IDC) from (Abate et al., 2016). Before calcination (SI), the freshly prepared catalyst showed the presence of in-homogeneously distributed spherical Pd NPs (Figure 1) with an average Pd NPs of 3.4±1.5 nm, typical of the sol immobilization procedure, as previously reported (Giorgianni et al., 2019). The average Pd NPs diameter is similar to the one obtained by IDC catalyst (Abate et al., 2016), although the SI catalyst's particle size distribution is narrower and bell-shaped (Giorgianni et al., 2019). The compared catalysts' exposed metal surface area decreases as SIC > IDC > NRC (Table 1). It must be considered that after calcination, the geometry of the particles might change slightly from spherical to a flatter geometry, similarly to what was observed for the IDC catalyst (Abate et al., 2016), here reported for comparison. Moreover, after calcination, the catalyst's visual color changed from black to pale-red, similarly to what reported by (Samanta, 2008), indicating the formation of surface PdOx species in interaction with Al_2O_3 in contrast with the formation of PdO (black-green). The latter phenomenon was also observed in the IDC catalyst case, which turned from black (metallic palladium) to red after calcination.

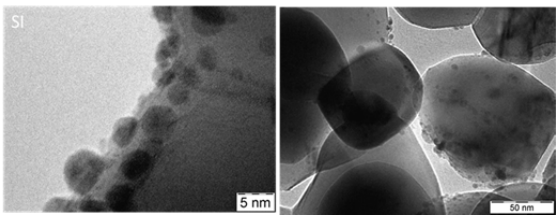

Figure 1: TEM Micrograph of the as-prepared catalyst (SI) catalyst.

Table 1: Average Pd NPs diameters and Pd Metallic Surface Areas (MSA) calculated assuming hemispherical particles from TEM Measurements

Cat.	Preparation Method	Calcination treatment	Pd Loading [mg]	Average Pd NPs diam. [nm] (s, [nm])	MSA [m^2/g]	Reference
SIC	Sol Immobilization	450°C, 1°C/min, 8h	4.2	3.4 (1.5)	113	This work
IDC	Impregnation-Decomposition	450°C, 1°C/min, 6h	4	3.8 (2.8)	73	(Abate et al., 2016)
NRC	Hydrazine Reduction	450°C, 1°C/min, 6h	3.5	12 (6.8)	23	(Abate et al., 2016)

3.2 Catalytic Performances

The fresh reduced SI catalysts (data not shown) showed, in the first three tests, an average selectivity at 240 min of 1.3, 4%, and 5% and a concentration of H_2O_2 at 240 min of 2.4, 3.6, and 4.6 mmol/L. The increasing selectivity and concentration of H_2O_2 with the time-on-stream of the catalyst have been previously related to transport problems within the PVA layer on the surface of Pd NPs (Giorgianni et al., 2019). Comparing the catalyst's performance in the presence of KBr with previous results, apparently, the presence of KBr together with the PVA layer further depresses the H_2O_2 productivity of the catalysts. Conversely, after calcination, SIC catalysts have shown a tremendous increase in selectivity (Figure 2 c).

Comparing the performance of the freshly calcined SIC catalyst with the performance achieved after the second testing cycle (Figure 2, Test 1 and 2), the concentration of H_2O_2, as a function of time (Figure 2 a), increased with a lower rate with respect to the second testing cycle. Similar behaviour was observed for the production rate of H_2O (Figure 2 b). Moreover, both the observed H_2O_2 and H_2O generation rates decreased as a function of time. Besides, the hydrogen conversion for the SIC catalyst (not shown), similar for both tests, decreased with the time on-stream from 26 (60 min) to 18 % (240 min). In the first test, the selectivity was stable at 69% over time, while, during the second test, it decreased to 58%.

Comparing the obtained result for the fresh SIC catalyst with the previously reported results of the NRC and IDC catalysts after calcination (Abate et al., 2016), showing a similar Pd loading (Table 1), the SIC catalyst showed the best selectivity. The productivity of H_2O_2 per gram of Pd, after 240 min, increased as NRC < SIC < IDC, while the productivity of H_2O increased as SIC < IDC < NRC. Also, with respect to IDC and NRC catalysts, which have shown an initial increase of both the rate H_2O_2 and H_2O, followed by a plateau for H_2O_2 and a continuous increase for H_2O rate, in the case of the SIC catalyst, this was followed by a decrease in the rate of formation of both H_2O_2 and H_2O, after about 1 hour of reaction time. Moreover, while the selectivity of the SIC catalyst was stable during each test, in the case of the NRC and IDC catalysts, it decreased monotonically during the time, while the generation rate of H_2O_2 and H_2O (Figure 2a and b) and hydrogen consumption rate increased (Figure 2 d). After postulating the inactivity of oxidized Pd, the latter phenomena were previously explained by an increased reduction degree of the catalyst with the reaction time, assuming

metallic Pd as the active site for the reaction (Abate et al., 2016). However, in the case of the SIC catalyst, showing a similar dispersion as the IDC catalyst, but calcined for a longer time than the latter (2 h more), the observed generation rate of H_2O_2 and H_2O cannot be explained by simply assuming an increasing reduction degree of the catalyst with the time on stream. Instead, the latter observations suggest an initial reduction of Pd's surface by the H_2 fed to the reactor, followed by a reoxidation of Pd by the generated H_2O_2. The latter was also confirmed by the catalyst's reddish colour, persisting even after further tests, suggesting the presence of oxidized palladium, in agreement with previous findings (Voloshin et al., 2008). The latter phenomenon was not observed for NRC and IDC catalysts, which, over a single test, turned from reddish to black after testing, indicating the reduction of the catalysts during the tests (Melada et al., 2006). The reoxidation of Pd, together with the presence of the large Pd surface area (Table 1), also explains the lower productivity of H_2O_2 and H_2O observed in the SIC catalyst case, with respect to both NRC and IDC catalysts. Moreover, the constant selectivity observed for the same catalyst during the second test suggests a negligible hydrogenolysis route's contribution.

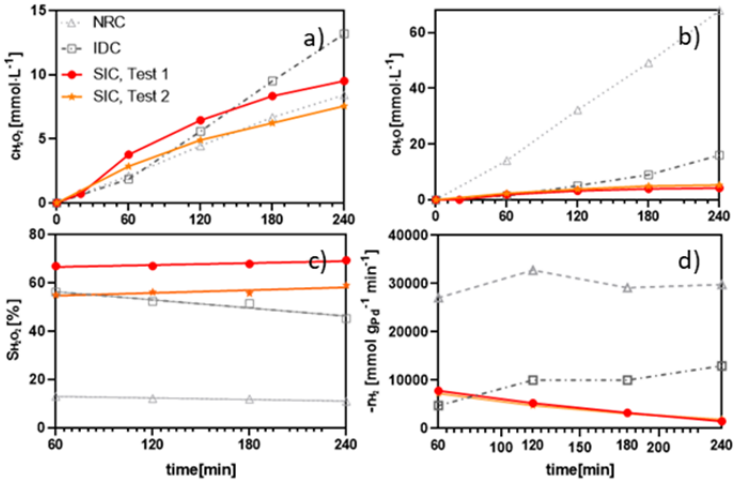

Figure 2: Comparison of the SIC with IDC and NRC catalysts (Abate et al., 2016) with respect to a) the formation of H_2O, b) H_2O, c) H_2O_2 selectivity, and d) H_2 consumption rate (r_{H_2}) as a function of time.

3.3 Kinetic Modelling

To better understand the observed generation rate of H_2O_2 and H_2O and the reason for the observed constant selectivity, a kinetic model was postulated.

In a previous paper (Abate et al., 2016), a new approach for modeling the kinetics of calcined palladium catalysts while taking into account the catalyst's redox behaviour was proposed (model 2, see model assumptions). Here, model-2 was modified assuming that: 1) the surface of oxidized Pd NPs is inactive for the synthesis while metallic Pd is the active site, and besides being reduced at the beginning of the tests and, as postulated in model-2 (Abate et al., 2016), can be oxidized by the formed H_2O_2 (Voloshin et al., 2008); 2) the hydrogenolysis route can be negligible in our experimental conditions and the corresponding pseudo-kinetic constant (k_h') was kept out for avoiding overfitting; 3) the direct synthesis (k_{ds}') and direct combustion (k_c') pseudo-kinetic constants are proportional to the reduced Pd surface. The new proposed model was formulated according to Eq(3)-Eq(6) (see symbols, definitions, and units).

$$\frac{dc_{H_2O_2}(t)}{dt} = S_r(t) \cdot S \cdot k'_{ds} \tag{3}$$

$$\frac{dc_{H_2O}(t)}{dt} = S_r(t) \cdot S \cdot k'_{c} \tag{4}$$

$$\frac{dS_r(t)}{dt} = k_{Pd,r} \cdot S \cdot \left(1 - S_r(t)\right) - k_{Pd,Ox} \cdot S_r(t) \cdot S \cdot c_{H_2O_2}(t) \tag{5}$$

$$S_r(0) = 0,\ c_{H_2O}(0) = 0,\ c_{H_2O_2}(0) = 0 \tag{6}$$

The proposed model was solved numerically by parametrizing the solution (LSODA algorithm) and fitted to the experimental data for H_2O and H_2O_2 by nonlinear regression (Levenberg-Marquardt algorithm) using Wolfram

Mathematica 10. Because the $k_{Pd,r}$ and $k_{Pd,Ox}$ constants were largely correlated with each other, $k_{Pd,r}$ was fixed and assumed to be the same as in the case of the IDC catalyst, presenting similar Pd dispersion (Abate et al., 2016). The fitting results were reported in Table 2.

Table 2: Pseudo-kinetic rate constants estimated for model-3 (see symbols, definitions and units)

Catalyst	Model	k_{ds}'	k_h'	k_c'	$k_{Pd,r\ (FIXED)}$	$k_{Pd,Ox}$	adj. R^2
SIC	3	0.305±0.07	-	0.14±0.03	0.108	0.056±0.02	0.998

The estimated pseudo-kinetic rate constant for the direct synthesis (k_{ds}') was not significantly different from the IDC catalyst and of the same order of magnitude as the previously reported data for NRC catalysts (Figure 3 a), indicating that the Pd surface is reduced at the beginning of the test, and then re-oxidized, as postulated by the mechanism. Conversely, the direct combustion rate (k_c') was 25% lower than the value obtained for the IDC catalyst, in line with the SIC catalyst's improved selectivity. Moreover, the assumption of a negligible contribution for the hydrogenolysis route (h) can be considered correct as the model predicts a constant selectivity. Comparing the inferred Pd surface reduction degree of the investigated catalysts, here expressed as the metallic fraction of the total surface of Pd NPs as a function of time-on-stream (Figure 3 b), the SIC catalyst, present a maximum degree of reduction of 55 %, while the surface reduction of IDC and NRC catalysts was complete at the end of the tests.

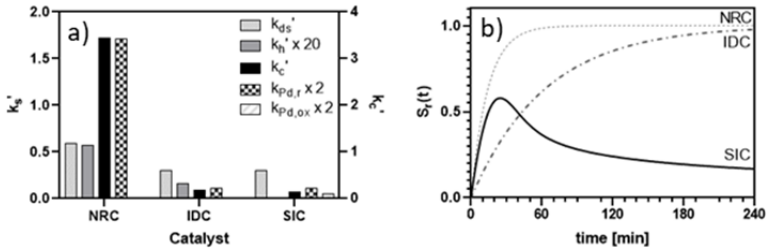

Figure 3: Comparison of the SIC with IDC and NRC catalysts from (Abate et al., 2016) a) with respect to the fitted pseudo-kinetic rate constants and b) estimated fractional surface reductio degree (S_r) as a function of the time on stream

The decreased Pd surface reduction rate of the IDC and SIC catalysts with respect to the NRC catalysts was related to Pd's increased interaction with the support, increasing with the series NRC < IDC < SIC, favoured by the large dispersion of Pd in IDC and SIC catalysts. The persistence of an oxidized Pd surface in the SIC catalyst, with respect to the IDC catalyst, was related to the prolonged calcination pre-treatment (8h) of the SIC catalyst with respect to the NRC and IDC catalysts (6 h) and was in line with the reddish colour of the SIC catalyst, persisting after further tests. Conversely, the IDC catalyst turned from reddish to black at the end of the test (metallic Pd). The observed decrease of the k_c' and k_h' constants in the series NRC > IDC > SIC were related to the structure-sensitivity of the direct combustion and hydrogenolysis reactions, requiring the presence of ensembles sites or kinks and corners sites of reduced Pd (Deguchi & Iwamoto, 2013), which are probably less abundant in the presence of a large degree of interaction with the support.

4. Conclusions

A structured catalyst was prepared by sol-immobilization and tested for the direct synthesis of H_2O_2 both in the reduced state (as prepared) and after calcination. After calcination, a marked increase in the selectivity toward H_2O_2 was shown. Moreover, the calcined catalyst, compared with the catalysts prepared by hydrazine-reduction and impregnation-decomposition after calcination, has shown stable activity overtime during the tests, indicating the negligible contribution of the H_2O_2 hydrogenolysis route. The shown performance overtime indicates an initial reduction of the calcined catalyst during the tests by the H_2 present in the reaction environment and further oxidation of the catalyst by the produced H_2O_2. The stabilization of the oxidized form of Pd, in interaction with the support, and the transient oxidation state of the surface of Pd, inferred by kinetic modeling, were related to the improved selectivity of the catalyst by considering the direct synthesis reaction as structure insensitive while considering the H_2O_2 hydrogenolysis and the direct combustion routes as structure-sensitive reactions.

5. Symbols, definitions, and units

$c_{H_2O_2}(t), c_{H_2O}(t)$: *concentration of H_2O and H_2O_2 expressed as* $\left[\frac{mmol}{L}\right]$

$\dot{n}_{H_2}(t)$: *molar flow of H_2, expressed as* $\left[\frac{mmol}{min}\right]$

$\varepsilon^t_{H_2}(t_0, t)$: *$H_2$ differential conversion between tome t_0 and t [-].*

V_{sln}: *testing solution volume, 100 mL.*

S: *total surface of Pd NPs as inferred by TEM measurements [m^2].*

$S_r(t)$: *fraction of the surface of Pd NPs in the reduced state [-].*

$k_{Pd,r}$: *pseudo-kinetic rate constant of reduction of the surface of Pd NPs* $\left[\frac{1}{min \cdot m^2}\right]$.

$k_{Pd,Ox}$: *pseudo-kinetic rate constant of oxidation of the reduced surface of Pd NPs* $\left[\frac{L \cdot m^{-2}}{mmol \cdot min}\right]$.

References

Abate, S, Melada, S., Centi, G., Perathoner, S., Pinna, F., & Strukul, G. (2006). Performances of Pd-Me (Me=Ag, Pt) catalysts in the direct synthesis of H_2O_2 on catalytic membranes. *Catalysis Today*, *117*(1–3), 193–198.

Abate, S., Arrigo, R., Schuster, M. E., Perathoner, S., Centi, G., Villa, A., Su, D., & Schlögl, R. (2010). Pd nanoparticles supported on N-doped nanocarbon for the direct synthesis of H_2O_2 from H_2 and O_2. *Catalysis Today*, *157*(1–4), 280–285.

Abate, S., Barbera, K., Centi, G., Giorgianni, G., & Perathoner, S. (2016). Role of size and pretreatment of Pd particles on their behaviour in the direct synthesis of H_2O_2. *Journal of Energy Chemistry*, *25*(2), 297–305.

Abate, S., Giorgianni, G., Gentiluomo, S., Centi, G., & Perathoner, S. (2015). Enhanced Hydrogen Transport over Palladium Ultrathin Films through Surface Nanostructure Engineering. *ChemSusChem*, *8*(22), 3805–3814.

Arrigo, R., Schuster, M. E., Abate, S., Giorgianni, G., Centi, G., Perathoner, S., Wrabetz, S., Pfeifer, V., Antonietti, M., & Schlögl, R. (2016). Pd Supported on Carbon Nitride Boosts the Direct Hydrogen Peroxide Synthesis. *ACS Catalysis*, *6*(10), 6959–6966.

Bianco, B., Macolino, P., & Vegliò, F. (2009). Optimization of Fenton's reagents by means of surface response model. Chemical Engineering Transactions, 17(January), 439–444.

Centi, G., & Perathoner, S. (2009). One-step H_2O_2 and phenol syntheses: Examples of challenges for new sustainable selective oxidation processes. *Catalysis Today*, *143*(1–2), 145–150.

Centi, G., Perathoner, S., & Abate, S. (2009). Direct Synthesis of Hydrogen Peroxide: Recent Advances. *Modern Heterogeneous Oxidation Catalysis: Design, Reactions and Characterization*, 253–287.

Choudhary, V. R., & Jana, P. (2008). Direct oxidation of H_2 to H_2O_2 over PdO/Al_2O_3 catalysts in aqueous acidic medium: Influence on H2O2 formation of Pd loading, calcination temperature and reduction of catalyst and presence of halide anions. *Catalysis Communications*, *9*(14), 2371–2375.

Deguchi, T., & Iwamoto, M. (2013). Catalytic Properties of Surface Sites on Pd Clusters for Direct H_2O_2 Synthesis from H_2 and O_2: A DFT Study. *The Journal of Physical Chemistry C*, *117*(36), 18540–18548.

Flaherty, D. W. (2018). Direct Synthesis of H_2O_2 from H_2 and O_2 on Pd Catalysts: Current Understanding, Outstanding Questions, and Research Needs. *ACS Catalysis*, 1520–1527.

Freakley, S. J., He, Q., Harrhy, J. H., Lu, L., Crole, D. A., Morgan, D. J., Ntainjua, E. N., Edwards, J. K., Carley, A. F., Borisevich, A. Y., Kiely, C. J., & Hutchings, G. J. (2016). Palladium-tin catalysts for the direct synthesis of H_2O_2 with high selectivity. *Science*, *351*(6276), 965–968.

García-Serna, J., Moreno, T., Biasi, P., Cocero, M. J., Mikkola, J.-P., & Salmi, T. O. (2014). Engineering in direct synthesis of hydrogen peroxide: targets, reactors and guidelines for operational conditions. *Green Chemistry*, *16*(5), 2320–2343.

Giorgianni, G., Abate, S., Centi, G., & Perathoner, S. (2019). Direct Synthesis of H_2O_2 on Pd Based Catalysts: Modelling the Particle Size Effects and the Promoting Role of Polyvinyl Alcohol. *ChemCatChem*, *11*(1), 550–559.

Iulianelli, A., Jansen, J. C., Esposito, E., Longo, M., Dalena, F., & Basile, A. (2019). Hydrogen permeation and separation characteristics of a thin $Pd\text{-}Au/Al_2O_3$ membrane: The effect of the intermediate layer absence. *Catalysis Today*, *330*, 32–38.

Melada, S., Rioda, R., Menegazzo, F., Pinna, F., & Strukul, G. (2006). Direct synthesis of hydrogen peroxide on zirconia-supported catalysts under mild conditions. *Journal of Catalysis*, *239*(2), 422–430.

Samanta, C. (2008). Direct synthesis of hydrogen peroxide from hydrogen and oxygen: An overview of recent developments in the process. *Applied Catalysis A: General*, *350*(2), 133–149.

Voloshin, Y., Halder, R., & Lawal, A. (2007). Kinetics of hydrogen peroxide synthesis by direct combination of H_2 and O_2 in a microreactor. *Catalysis Today*, *125*(1–2), 40–47.

Voloshin, Y., Manganaro, J., & Lawal, A. (2008). Kinetics and Mechanism of Decomposition of Hydrogen Peroxide over Pd/SiO_2 Catalyst. *Industrial & Engineering Chemistry Research*, *47*(21), 8119–8125.